ELSEVIER

Nuclear Instruments and Methods in Physics Research B 172 (2000) 193–200

NIM B
Beam Interactions with Materials & Atoms

www.elsevier.nl/locate/nimb

Minicyclotron (SMCAMS)-based accelerator mass spectrometry and real ^{14}C measurements

Maobai Chen [a,*], Xiangshun Lu [a], Deming Li [a], Yonghao Liu [a], Weijian Zhou [b], Guosheng Chen [a], Ligong Shen [a], Senlin Xu [a], Yuexiang Zhang [a]

[a] *Shanghai Institute of Nuclear Research, Chinese Academy of Sciences, P.O. Box 800204, Shanghai 201800, People's Republic of China*
[b] *Xian Laboratory of Loess and Quaternary Geology, Chinese Academy of Sciences, Xian 710054, People's Republic of China*

Abstract

The significant progress of the Shanghai minicyclotron-based accelerator mass spectrometer (SMCAMS) will be described in the research of accelerator mass spectrometry combined with the development of facility performance. The first real ^{14}C measurements were performed and an excellent agreement was obtained in an intercomparison of samples measured at SMCAMS and at tandem AMS facilities.

1. Introduction

The Shanghai minicyclotron-based accelerator mass spectrometer (SMCAMS) has been put into routine application by the radiocarbon community since 1 January 1999, after having been arduously explored for 10 years (excluding three years of feasibility study in advance) because of unexpected difficulties and hardships in both technique and funds. A schematic view of the SMCAMS in its present form is shown in Fig. 1. Since the completion of construction of this new type of minicyclotron [1], we had devoted our energy to exploring an effective method for precise radiocarbon measurements on the minicyclotron-based AMS facility for more than five years, owing to its different principles of radiocarbon analysis as compared to the tandem-based AMS facility. Research on accelerator mass spectrometry on the SMCAMS was carried out from two aspects: (1) refinement of the methods for ^{14}C analysis and (2) parameterization of the factors causing ^{14}C fractionation. In the meantime, endeavors in three aspects continuously proceeded during the past years [2]: (1) design, test and improvement of the home-made vertical multisample device for the vertical ion source; (2) development of software and hardware for sequential acceleration; and (3) improvement of the performance of the whole facility. Based on the achievements in both refinement of methods and improvement of equipment, we have successfully measured [3] on the SMCAMS the first real unknown samples of both archaeology and ancient geology, and satisfactory results have been

* Corresponding author. Tel.: +86-21-5955-3998; fax: +86-21-5955-3021.
E-mail address: smcams@sinr.ac.cn (M. Chen).

0168-583X/00/$ - see front matter
PII: S0168-583X(00)00390-6

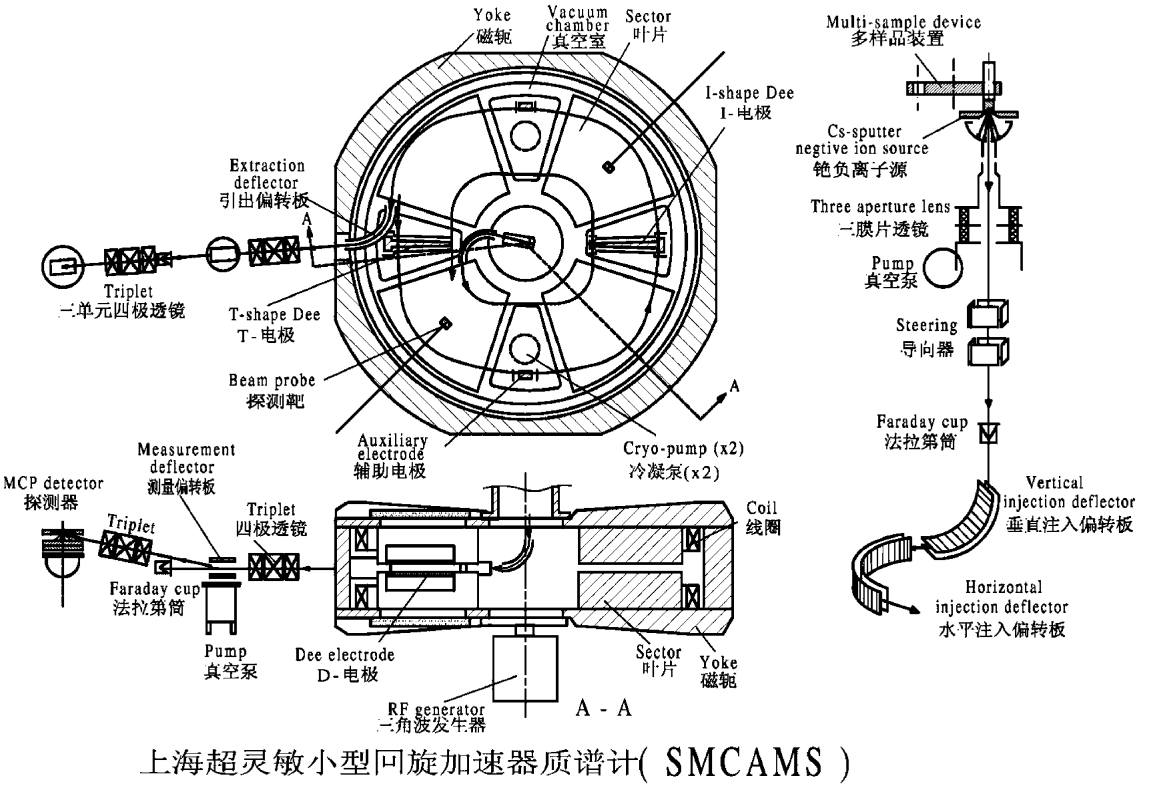

Fig. 1. Scheme of the Shanghai minicyclotron-based accelerator mass spectrometer (SMCAMS).

confirmed after intercomparison with Arizona University and Beijing University.

2. Refinement of the methods for ^{14}C analysis

For ^{14}C analysis, one must measure the ratio between carbon isotopes, such as $^{14}C/^{12}C$, $^{14}C/^{13}C$ or $^{13}C/^{12}C$. However, it is impossible for the minicyclotron to simultaneously accelerate ions with different masses. Therefore, the carbon ions must be accelerated and measured sequentially. Different sequential acceleration schemes were tested during the research of minicyclotron-based accelerator mass spectrometry.

2.1. Carbon isotope (C)-sequential acceleration

In C-sequential acceleration, $^{14}C^-$, $^{13}C^-$ and $^{12}C^-$ from the same sample are sequentially accelerated. However, it is more difficult to carry out the sequential acceleration for minicyclotron AMS than for tandem AMS because (1) according to the similarity theory of orbit, most of the power supplies must alternately be changed by 15% due to the mass difference of 15% between ^{14}C and ^{12}C; consequently, (2) the status of the minicyclotron facility is always under a prompt change, which is contradictory to the strict demand for high stability of all electric parameters; and (3) the frequently and swiftly changing r.f. voltage inevitably causes electromagnetic induction in the magnet coils, which seriously deteriorates the stability of the magnet power supply.

2.2. Sample(S)-sequential acceleration

As an alternative to the C-sequential acceleration, we tried the so-called S-sequential acceleration, which was described in AMS-7 [2]. The

electrical parameters are first set to optimum for $^{12}C^-$ acceleration, and the ^{12}C measurements of all samples proceed consecutively. Then the electrical parameters were changed to optimal values for $^{13}C^-$ and then for $^{14}C^-$ acceleration in the same manner. Such a sample-alternating measurement is entirely different from the particle-alternating scheme. Its total measuring time is prolonged, since the sample rotating time increases twofold, and it is certainly inadequate for measurement of a large quantity of samples. In addition, the long period between isotope ratio measurements reduces reproducibility.

2.3. Frequency (F)-sequential acceleration

In order to avoid rapid changing of most power supplies, F-sequential acceleration was tested to sequentially accelerate $^{14}C^-$, $^{13}CH^-$ and $^{12}CH_2^-$, in which only the radio frequency needed to be changed. However, very few experiments were carried out on it because the beam intensity of $^{12}CH_2$ declined more rapidly than that of ^{13}CH. This made the ratio of ^{13}CH to $^{12}CH_2$ continuously rise for far more than 1 h (Fig. 2), leading to nonreproducibility of the measured ratio of $^{13}CH/^{12}CH_2$. Therefore, the presumption that the probabilities of combining ^{12}C with H_2, and ^{13}C with H, will be unchanged when the content of H in or around the samples changes is incorrect.

2.4. Hydrogen (H)-sequential acceleration

Occasionally, H-sequential acceleration was tested, in which $^{12}CH^-$ and $^{13}CH^-$ were sequentially accelerated. Although it is doubtful whether the ratio $^{13}CH/^{12}CH$ can represent the ratio $^{13}C/^{12}C$ of the various samples themselves, experiments showed that the ratio $^{13}CH/^{12}CH$ was very stable as well as identical among the same kind of samples, even though their beam intensities rapidly declined (Fig. 3). Such experiments have shown us that the measured ratio will be very stable if the measured beam intensities are weak enough. We were also reminded of the fact that the beam current of $^{12}C^-$ in the SMCAMS facility has never exceeded 750 nA, even if the beam current of $^{13}C^-$ has reached 30 nA (the corresponding beam current of $^{12}C^-$ should have been around 3000 nA). Unexplained factors, maybe large emittance, poor local vacuum, or strong space charge effects arising from high beam intensity of $^{12}C^-$, must have deteriorated the ^{12}C beam, causing the fluctuations and nonreproducibility of the measured $^{13}C/^{12}C$ ratio.

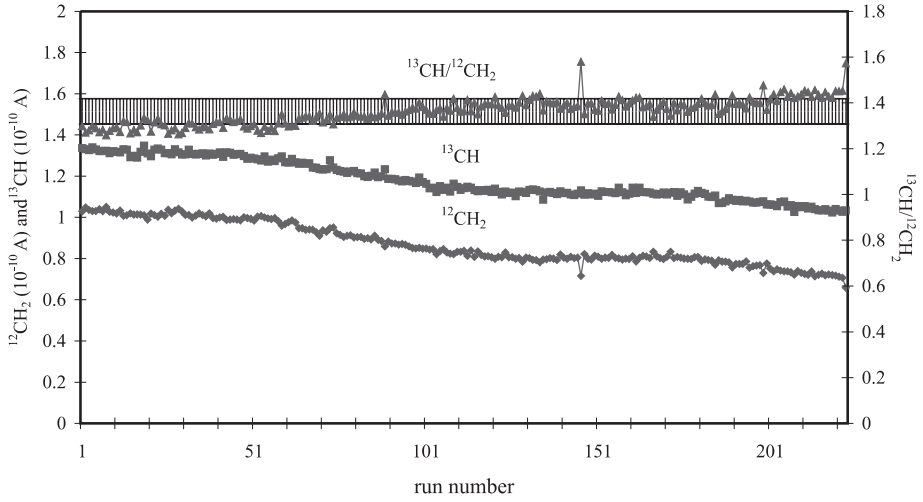

Fig. 2. ^{13}CH, $^{12}CH_2$ and $^{13}CH/^{12}CH_2$ versus cycle number during F-sequential acceleration.

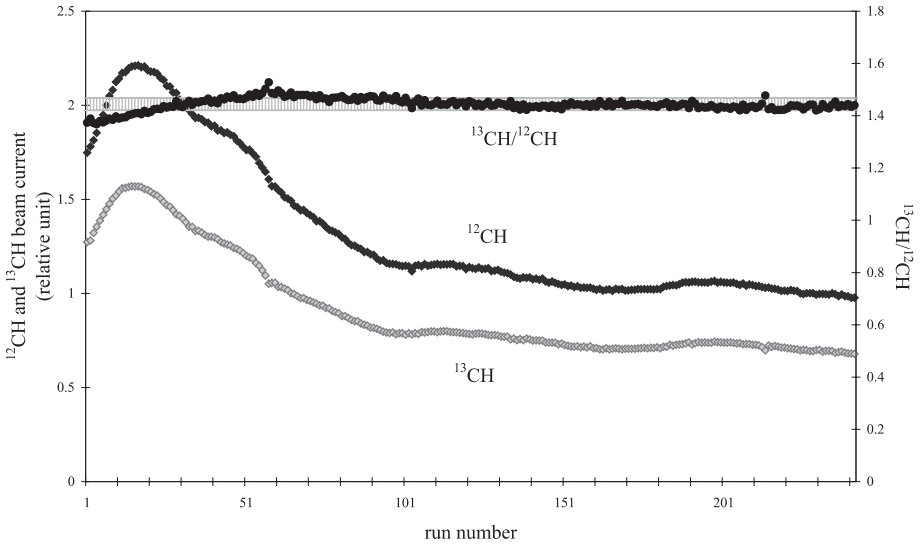

Fig. 3. ^{13}CH, ^{12}CH and ^{13}CH/^{12}CH versus cycle number during H-sequential acceleration.

2.5. Adopted (A)-sequential acceleration

Finally, A-sequential acceleration was tested, in which we only measured weak beams of $^{14}C^-$ and $^{13}C^-$ from enriched samples instead of accelerating high intensities of $^{12}C^-$ (as in the C-sequential acceleration). Happily, satisfactory results were reached during A-sequential acceleration (Fig. 4). Hence, the A-sequential acceleration is now adopted for real ^{14}C measurements.

2.6. X-ray background (X)-sequential acceleration

Before we solved the strong X-ray background problem, we introduced the X-background (X)-sequential acceleration, in which X-ray-induced background was sequentially measured along with ^{14}C and ^{13}C measurements. The net ^{14}C counts were obtained by subtracting the measured X-ray spectrum from the measured ^{14}C spectrum. This method not only increased the total measuring

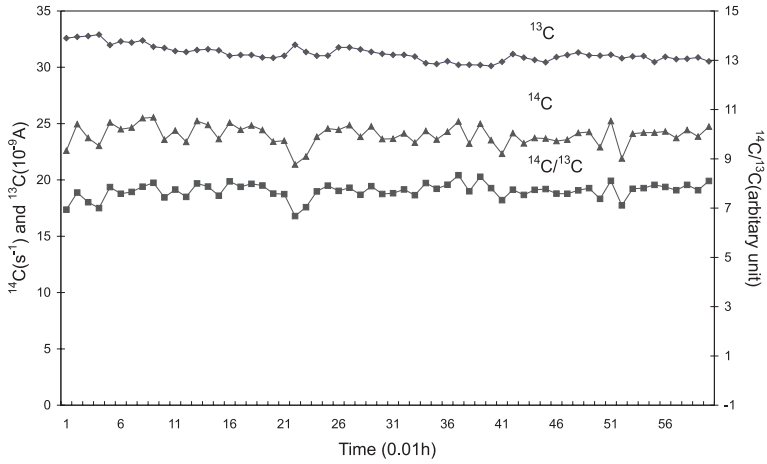

Fig. 4. ^{13}C, ^{14}C and ^{14}C/^{13}C versus cycle number during A-sequential acceleration, where the maximum ^{14}C counting rate reached is about 25 cps measured in 60 cycles with each 40 s by consecutively rotating samples three times.

time by a factor of two, but also introduced a larger error because the fluctuation of the X-background was over 10%. The X-sequential acceleration method is especially inadequate for ancient samples with very low ^{14}C content.

3. Parameterization of the factor causing ^{14}C fractionation

3.1. Fluctuation of electrical parameters

The formidable obstacle to acquiring flat-top transmission in the minicyclotron was one of the main factors causing fractionation. Although the apertures of all lens, steering and accelerating (Dee) electrodes and deflector channels were enlarged to the greatest possible width, the transmission through the injection and extraction deflectors channels was still very sensitive to fluctuations in the deflector voltage and to the orbit of the beam entering them.

3.2. Setting of operation parameters

To maximize the ^{14}C counting rate, we first optimized the $^{13}CH^-$ beam measured at the dynode of the MCP detector with -3 V voltage applied. Then the similarity theory of orbit served as the basis for scaling the operation parameters for other ions with different mass to operate them with similar orbit. This was both effective and convenient, but did not correspond to their respective optimal parameter setting, which was often too critical to stabilize their own operation. Despite this, these scaled orbits induced less fractionation than orbits formed by individually optimizing parameters for individual ion beams.

3.3. Positioning and cratering of samples

The reproducibility of the positioning of the samples on the home-made vertical multisample device played an important role in reducing fractionation, which forced us to spend significant effort in verifying that both coincidence and reproducibility of the sample position matched within 0.04 mm [2].

The cratering effect of the sample surface was more crucial in minicyclotron AMS than in tandem AMS. We tested various procedures of sample pressing to make the surfaces of the samples as identical as possible and to extend their lifetime.

3.4. Difference of emittance of the injected beam

The first electrode of the three-aperture lens constitutes the extraction electrode of the Cs sputter negative-ion source. To become a single lens, the first (extraction) electrode of the three-aperture lens was electrically connected with the third electrode, to which a voltage was applied to adjust the injection energy of ions entering the minicyclotron. Consequently, with the change of the injection energy of ions during sequential acceleration, the emittance of the ions was different due to their different extraction energies. Likewise, owing to their different injection energies but identical injection momentums to match the fixed injection magnetic rigidity of ions at the injection radius of the minicyclotron, the injection emittances of ion beams with different masses were also quite different. Such emittance differences induce fractionation.

3.5. Local vacuum at the surface of accelerator parts

The vacuum, especially the local vacuum, in the acceleration chamber of the minicyclotron seriously affected (Fig. 5) the loss of heavy negative ions with both extra-low energy (<50 KeV) and long pathways (~200 m). Due to the lack of an analyzing magnet prior to the minicyclotron, all particles were simultaneously injected into the vacuum chamber during sequential acceleration [4]. The vacuum read by the vacuum gauge at the side of the vacuum chamber mainly depended on the intensity of injected $^{12}C^-$ and C_2 beams while accelerating $^{13}C^-$ or $^{14}C^-$ ions. Consequently, during $^{13}C^-$ acceleration, the different ^{13}C beam intensities of the samples were not reflected in the readout of the vacuum gauge, but nevertheless resulted in different local vacuum near the surface of accelerator parts hit by the lost $^{13}C^-$ ions. This

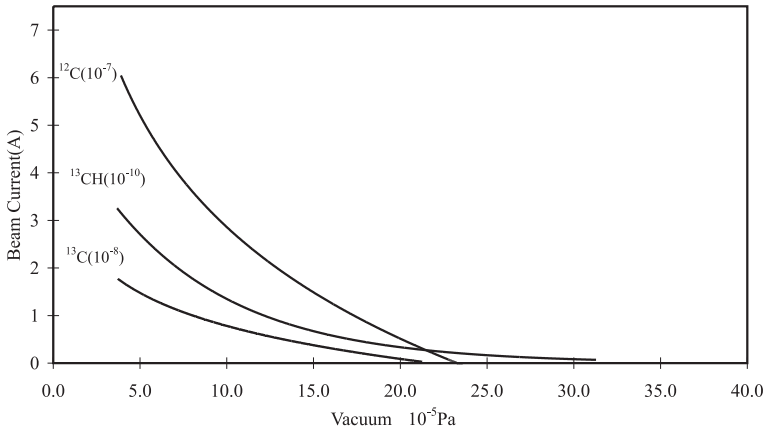

Fig. 5. Beam current of ^{12}C, ^{13}C and ^{13}CH versus vacuum in the SMCAMS.

could induce fractionation of ^{13}C, because the $^{14}C^-$ beam is probably too weak to induce significant local vacuum change.

3.6. The stray electric field around the three deflectors

In the acceleration chamber of the minicyclotron, the stray electric field of the three deflectors [4] seriously affected the orbit of particles with extra-low energy. After having shielded all the deflectors on which the high voltage was applied, the beam intensity was increased by a factor of two, and the beam stability was improved considerably. However, the electric field penetrating from both the exit of the horizontal injection deflector and the entrance of the horizontal extraction deflector could not be shielded completely (Fig. 6), which might still induce fractionation.

3.7. X-ray interference to the MCP detector

The acceleration chamber of the minicyclotron is an intense source of X-rays [5]. X-rays cannot be discriminated by the MCP detector and would introduce a strong background in the total ^{14}C spectrum (Fig. 7(a)). Lead shielding could not entirely suppress the X-ray background, and the interference got stronger with improved facility performance (beam intensity). Fortunately, we recognized that there were no X-ray counts in the MCP detector when the voltage on the vertical injection deflector was off and all injected particles did hit the entrance. This implies that even strong X-rays produced above the median plane of the minicyclotron have no effect on the MCP detector located at the median plane outside the minicyclotron. Inspired by this discovery we moved the MCP detector 20 cm above the median plane (Fig. 1). The X-ray interference was thus reduced by a factor of 20 (Fig. 7(b)). So its influence on ^{14}C measurement was negligible.

4. Intercomparison of the first real ^{14}C measurements

Based on the achievements of both the research of accelerator mass spectrometry and the improvement of the facility performance, we made the first attempt in September and October 1998 to carry out ^{14}C measurement of real samples. The results of these measurements, which comprised seven archaeological samples 2000–3000 years old and two of ages near 30 000 years are presented in the paper by Zhou et al. [3] in these proceedings. The measured results were unexpectedly satisfactory as compared with those measured by Arizona University and Beijing University, even though it

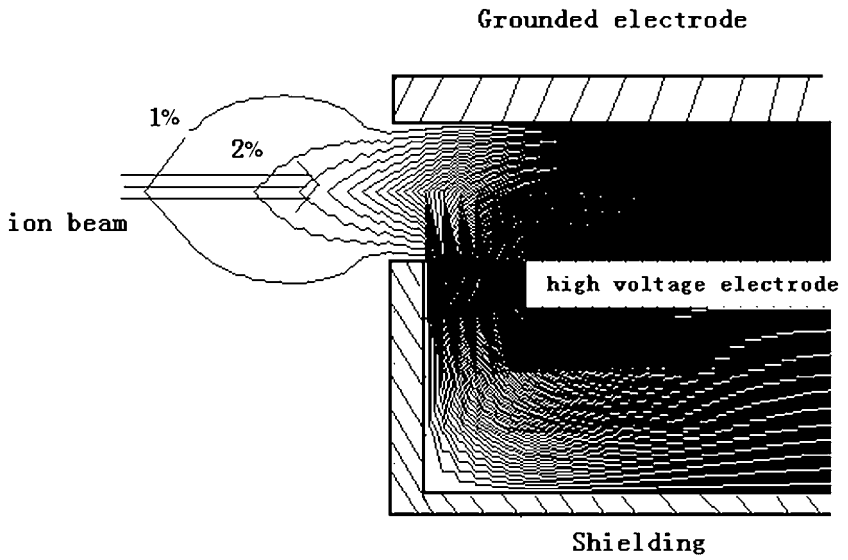

Fig. 6. The calculated distribution of the electric potential penetrating from the exit (entrance) of the horizontal injection (extraction) deflector with full shielding.

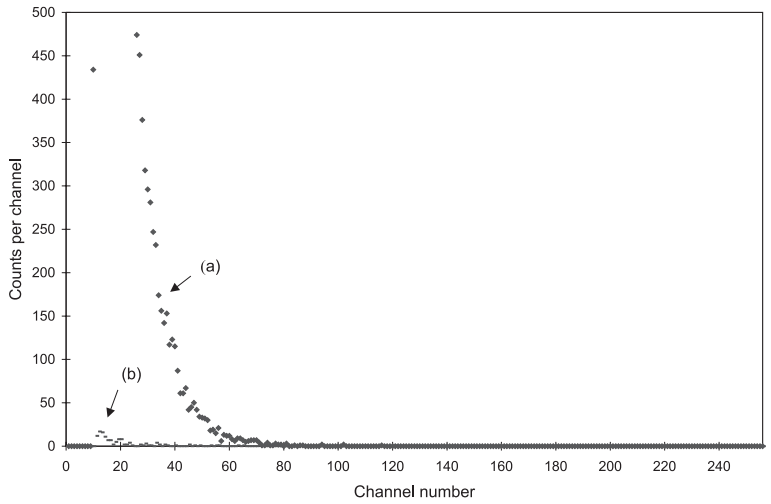

Fig. 7. The X-ray background spectrum measured (a) before and (b) after the MCP detector was moved away from the median plane of the minicyclotron by 20 cm. In (a), the strong X-rays could not be discriminated by the MCP detector and were recorded at the low channels (low pulse height due to the low X-ray energy) of the multi-channel pulse analyzer. Originally, the peak of the X-ray spectrum was located at about channel 10, but its tail extended to higher channels and was mixed with ^{14}C counts. Consequently, we had to set the pulse-height threshold at a higher channel close to the peak of the measured ^{14}C spectrum to eliminate X-ray interference. As a result, not only did the detecting efficiency of the MCP reach only 60% or so, but also, the ^{14}C counting fluctuation, which occurred around the threshold channel, introduced a counting error into the total ^{14}C counts. In (b), the X-ray interference was suppressed by a factor of 20. Subsequently, the pulse-height threshold could be set at channel 15–20, well away from the peak of the ^{14}C spectrum, and the detecting efficiency increased to 95–98%. So, the fractionation of ^{14}C was negligible.

was the first time we made real ^{14}C measurements with our new type of AMS facility.

The intercomparison of our results with the ones from Arizona University and Beijing University showed agreement within one to two sigma [3]. The ^{14}C counting rate for the standard sample made from Chinese sugar (1.36 times modern carbon) reached 20–25 cps on the mini-cyclotron AMS (Fig. 2).

It is obvious from the results in [3] that the performance of the SMCAMS facility is now sufficient for its practical application in biomedical science, environmental science, archaeology and geoscience and it has been opened to the radiocarbon community since early this year. OUR International Tech. & Sci. (Shenzhen, China) is interested in industrializing the SMCAMS facility for the world.

Acknowledgements

This work is supported by the Chinese Academy of Science, the National Natural Science Foundation of China, the Shanghai Municipal Science and Technology Committee, the International Atomic Energy Agency, and OUR International Tech. & Sci. Co. Ltd.

References

[1] M.B. Chen et al., Nucl. Instr. and Meth. B 92 (1994) 213.
[2] M.B. Chen et al., Nucl. Instr. and Meth. B 123 (1997) 102.
[3] W.J. Zhou, M.B. Chen, Y.H. Liu, D. Donahue, J. Head, X.F. Lu, A.J.T. Jull, Nucl. Instr. and Meth. B 172 (2000) 201.
[4] M.B. Chen et al., in: Proceedings of the 14th Conference on Cyclotrons and their Applications, 1995, p. 107.
[5] M.B. Chen et al., Radiocarbon 37 (1995) 675.